Journal of Materials Chemistry B

RSC Publishing

PAPER

View Article Online
View Journal | View Issue

Chitosan and chitosan–ZnO-based complex nanoparticles: formation, characterization, and antibacterial activity

Cite this: *J. Mater. Chem. B*, 2013, **1**, 1968

Ilana Perelshtein,[a] Elena Ruderman,[a] Nina Perkas,[a] Tzanko Tzanov,[b] Jamie Beddow,[c] Eadaoin Joyce,[c] Timothy J. Mason,[c] María Blanes,[d] Korina Mollá,[d] Anitha Patlolla,[e] Anatoly I. Frenkel[e] and Aharon Gedanken*[a]

Received 20th December 2012
Accepted 4th February 2013

DOI: 10.1039/c3tb00555k

www.rsc.org/MaterialsB

Nanostructured chitosan (CS) and a chitosan–Zn based (Zn–CS) complex have been synthesized and simultaneously deposited on cotton fabrics using ultrasound. SEM measurements revealed that the coating consists of nanoparticles (NPs) of *ca.* 40 nm in diameter, homogeneously dispersed along the yarns. XANES studies pointed out that the complex consisted of a less than 2.1 nm ZnO core to which the chitosan was bonded. Additionally, FTIR measurements indicated the *in situ* formation of a Zn–CS complex which is the only deposited material on the cotton surface. The antibacterial properties of the CS and Zn–CS coated textiles were tested against Gram positive and Gram negative bacteria species. More than two-fold increase of the antibacterial activity of Zn–CS NP coated textiles was detected as compared to the fabrics treated with the sonochemically synthesized CS NPs alone. The sonochemical technique appears to be a suitable method for producing organic NPs of soluble compounds, without loss of their intrinsic properties, *i.e.* the antimicrobial activity of chitosan. Moreover, hybrid nanoorganometallic particles were simultaneously synthesized and deposited on cotton sonochemically.

Published on 04 February 2013 on http://pubs.rsc.org | doi:10.1039/C3TB00555K
Downloaded by BNL Research Library on 25 March 2013

1 Introduction

Chitosan, a polysaccharide composed of glucosamine and *N*-acetyl-glucosamine units, is well known for its antibacterial properties. Due to its biodegradability, biocompatibility, and lack of toxicity, CS in the bulk form has found numerous applications as an antibacterial coating for textiles.[1–7] Recently, Fana *et al.* reported on the preparation of chitosan nanoparticles (NPs) by a novel method based on ionic gelation using sodium tripolyphosphate (TPP).[8] Wazed *et al.* have further demonstrated the advantage of using NPs instead of bulk chitosan in order to enhance the antibacterial activity of coated textiles.[9]

Additionally, the combination of CS with inorganic NPs was an efficient approach to produce antibacterial materials with improved functional properties. It has been reported that the nanosilver– and silver zeolite– or silver hydroxoapatite–CS composites provide increased mechanical strength and water barrier properties.[10,11] Improved mechanical properties and superior inhibition of bacterial growth have been observed for porous CS–silver nanocomposite films.[12] The enhanced antibacterial activity of the CS–Ag–ZnO composite has also been demonstrated.[13] Recent studies on ZnO–CS complexes in the form of films, membranes and dyes have indicated that the presence of ZnO NPs significantly improved the antibacterial properties of CS.[14,15] The advantages of combining CS with ZnO NPs as an alternative to the widely used Ag NPs reside in their lower cost, lack of color and UV-blocking properties.[16]

Reports for preparing ZnO–CS nanocomposites are based on the conversion of ZnO into an ionic form followed by complexation with CS in solution under continuous stirring.[14,15] Coating methods for application of a ZnO–CS composite on cotton fabrics consist of carboxymethylation of CS followed by reaction with zinc sulfate in concentrated sodium hydroxide.[17]

In our previous work ultrasound has been used for coating textiles with antibacterial inorganic NPs. The synthesis and deposition of these NPs were performed simultaneously under sonication resulting in strong adherence to the surface of the fibrous substrate.[18–20] The aim of the present work was to demonstrate the feasibility of the sonochemical coating of textiles with CS NPs and a CS–Zn nanocomposite in a single-step process without the use of any binding agents. The effect of

[a]*Department of Chemistry, Kanbar Laboratory for Nanomaterials, Institute of Nanotechnology and Advanced Materials, Bar-Ilan University, Ramat-Gan 52900, Israel. E-mail: Aharon.Gedanken@biu.ac.il; Ilana.Perelshtein@biu.ac.il; rulena@gmail.com; Nina.Perkas@biu.ac.il*

[b]*Universitat Politècnica de Catalunya, Edifici Gaia, Pg. Ernest Lluch/Rambla Sant Nebridi s/n, 08222 Terrassa, Spain. E-mail: tzanko.tzanov@upc.edu*

[c]*Sonochemistry Centre, Faculty of Health and Life Sciences, Coventry University, Coventry CV1 5FB, UK. E-mail: j.beddow@coventry.ac.uk; e.joyce@coventry.ac.uk; t.mason@coventry.ac.uk*

[d]*Textile Research Institute, AITEX, Plaza Emilio Sala, 1, 03804 Alcoy, Spain. E-mail: mblanes@aitex.es; kmolla@aitex.es*

[e]*Physics Department, Yeshiva University, New York, NY 10016, USA. E-mail: patolla@yu.edu; Anatoly.Frenkel@yu.edu*

This journal is © The Royal Society of Chemistry 2013

Published on 04 February 2013 on http://pubs.rsc.org | doi:10.1039/C3TB00555K
Downloaded by BNL Research Library on 25 March 2013

the combination of CS and Zn on the antimicrobial activity of the coated textile surfaces is discussed in this paper. To the best of our knowledge, this is the first study describing the deposition of organometallic nanocomposites on fabrics in a one-step sonochemical process. The study is also the first demonstration that ultrasonic waves are able to form NPs of an organic water-soluble compound without the use of a surfactant or any other mediation product.

2 Experimental

Different types of fabrics such as polyester, cotton and cotton–polyester supplied by Klopman Int. (Italy) have been used in the experiments. Independently of the fabric composition, the coating quality on all materials was the same, and thus only the results obtained on cotton are reported here. All chemicals from Sigma Aldrich were of analytical grade, and used without further purification. Low molecular weight CS (15 kDa) from Kitozyme S.A. (Belgium), $Zn(CH_3COO)_2 \cdot 2H_2O$ and aqueous solution of ammonia (28 wt%) were used in the experiments.

Oxoid plate count agar (PCA), nutrient agar (NA) and nutrient broth (NB) were purchased from Fisher Scientific, UK. For the preparation of the neutralising medium (SCDLP), casein peptone and soybean peptone were purchased from Sigma-Aldrich. Analytical grade NaCl, KH_2PO_4, NaOH, D-glucose, lecithin and Polysorbate 80 were purchased from Fisher Scientific (UK). Deionised water was used for preparation of all solutions.

2.1 Chitosan NPs formation and deposition on cotton

CS (30 mg) dissolved in 1 ml of 1% aqueous acetic acid was added to a mixture of 10 ml water and 90 ml ethanol. The reaction slurry was irradiated for 1 h with a high-intensity ultrasonic horn (Ti horn, 20 kHz, 750 W at 24% efficiency) in a thermostatted (30 °C) sonicator cell during the reaction (1 h). The reaction was carried out in the presence of a 10 × 10 cm sample of cotton fabric in the cell. At the end of the process, the fabric was washed with water and ethanol and dried under vacuum before being analyzed.

2.2 Synthesis and deposition of Zn–CS hybrid NPs on cotton

CS (30 mg) was dissolved in 1 ml of 1% aqueous acetic acid. Zinc acetate (0.022 g) was dissolved in 10 ml water and 90 ml ethanol, and added to the CS solution. The reaction mixture, in which pH was adjusted to 8 by dropwise addition of 25% aqueous ammonia, was sonicated in the presence of a 10 × 10 cm fabric sample for 1 h at 30 °C as described above. Thereafter, the fabric was washed with water and ethanol and dried under vacuum.

2.3 Antibacterial activity testing

The antibacterial efficacy of the treated fabrics was determined using the absorption method from BS EN ISO 20743:2007 (Anon 2007). Antimicrobial tests were carried out with two bacterial species: Gram positive *Enterococcus faecalis* (NCIMB 775) and Gram negative *Escherichia coli* (ATCC 8739). Overnight cultures of each of the bacteria were grown in nutrient broth (NB, Oxoid) in a shaking incubator at 37 °C and 110 rpm. Following this incubation, a 0.4 ml aliquot was transferred to 20 ml of fresh sterile NB and incubated for 3 h at 37 °C and 110 rpm. This 3 hour culture was then diluted 3-fold in dilute nutrient broth (1 : 20 dilution in water) to give a bacterial suspension with between 1×10^5 and 3×10^5 colony forming units per ml (CFUs per ml).

For each bacterial strain, 0.4 g pieces of control fabric and 0.4 g pieces of the coated test fabric were inoculated with 0.2 ml of the dilute bacterial suspension. The bacterial suspension was added dropwise to each fabric sample in order to allow it to be fully absorbed. Thereafter, the control samples and test samples were placed in an incubator at 37 °C in capped vials. Furthermore, control and test samples were immediately mixed with 20 ml of a neutralising medium (soybean casein digest lecithin polysorbate medium, SCDLP). The resulting suspensions of bacteria were serially diluted in NB to 10^{-5}. One ml of each dilution was mixed with 17 ml of molten plate count agar (PCA, Oxoid) and allowed to set in a sterile Petri dish. All plating was carried out in duplicate. The agar plates were then incubated for 24 ± 4 h at 37 °C. The number of colonies on the plates after incubation was counted for determination of the inoculum cell density (CFUs per ml). The remaining control and test pieces were incubated with the absorbed bacterial suspensions for between 18 and 24 h at 37 °C, then shaken with SCDLP and plated as described above. The number of colonies on these plates was used to determine the level of bacterial growth on the control and test fabrics. The antibacterial efficiency value (A) was calculated using the following formula:

$$A = F - G \quad (1)$$

where F = growth value on the control fabric sample ($\log_{10}$ CFU per ml post incubation − $\log_{10}$ CFU per ml prior to incubation) and G = growth value on the NP treated fabric samples ($\log_{10}$ CFU per ml post incubation − $\log_{10}$ CFU per ml prior to incubation).

2.4 Characterization

The Zn^{2+} content on the coated fabric was determined by inductively coupled plasma (ICP) analysis using a ULTIMA JY2501 instrument. The morphology and size of the NPs were studied with an environmental scanning electron microscope (ESEM), model Quanta 200FEG of FEI. The coated fabrics were further characterized by Fourier transform infrared spectroscopy (FTIR) using a Tensor 27 FTIR spectrometer (Bruker, Germany), performing 100 scans for each spectrum. No smoothing function or baseline correction was applied. Potassium bromide was used to obtain the background spectrum. The presence of N and Zn atoms on the coated fabrics was evaluated by X-ray Photoelectron Spectroscopy (XPS) using monochromatized Al Kα radiation (Kratos, Japan). The X-ray diffraction (XRD) patterns of the materials were measured with a Bruker D8 diffractometer (Karlsruhe, Germany) using Cu Kα radiation. X-ray absorption fine structure (XAFS) spectroscopy experiments were performed at the X18B beamline of the National Synchrotron Light Source. X-ray detectors for transmission measurements were gas-filled ionization chambers. A PIPS

Published on 04 February 2013 on http://pubs.rsc.org | doi:10.1039/C3TB00555K
Downloaded by BNL Research Library on 25 March 2013

detector was used for fluorescence measurements. Up to five energy scans were measured and averaged to optimize the signal to noise ratio. Zn foil was positioned between the transmission and reference detectors and its absorption coefficient was measured simultaneously with the main sample for energy calibration and alignment.

3 Results and discussions

3.1 Structural and morphological studies

3.1.1 XRD. The solid precipitates in the sonication cell after: (i) the sonochemical deposition of dissolved CS, and (ii) the simultaneous reaction between dissolved CS and zinc acetate solution, were analyzed by XRD. Identical patterns were obtained for both samples revealing the presence of an amorphous compound (Fig. 1a). One of the possible pathways for the reaction between a solution of CS and zinc acetate is the formation of a crystalline ZnO phase in parallel with the CS precipitation on the cotton. A crystalline hexagonal ZnO structure was detected in our previous study involving the formation and simultaneous deposition of ZnO NPs by ultrasound.[20] Fig. 1b shows the diffraction peaks for ZnO obtained from the hydrolysis of zinc acetate. However, despite the same reaction conditions as in ref. 20 have been used in the current study, the characteristic peaks of crystalline ZnO could not be observed in the XRD pattern of the hybrid Zn–CS coating. The absence of crystalline ZnO phase indicates either the nanoscale dimension of ZnO nanocrystals or the formation of an amorphous Zn–CS composite. This ambiguity prompted us to investigate the local structure around Zn by XAFS analysis (*vide infra*).

3.1.2 XAFS. X-ray absorption near-edge structure (XANES) and extended XAFS (EXAFS) measurements are excellent tools to investigate the electronic structure and geometry in the nearest coordination environment around X-ray absorbing atoms. Fig. 2 shows the Zn K-edge XANES data in the Zn–CS system and relevant Zn-containing compounds with known electronic and crystallographic structure: $Zn(Ac)_2$ and two samples of ZnO nanocrystals with 2.1 and 300 nm size, respectively. The latter data were obtained and published.[21] The shape and position of the 1s–4p absorption peak maximum in ZnO NPs strongly depend on the particle size. Absorption shift to a higher energy was observed for 300 nm particles compared to the 2.1 nm ones (Fig. 2 and ref. 21), in agreement with the theoretical calculations of Kuzmin *et al.*[22] As expected, the shape and peak

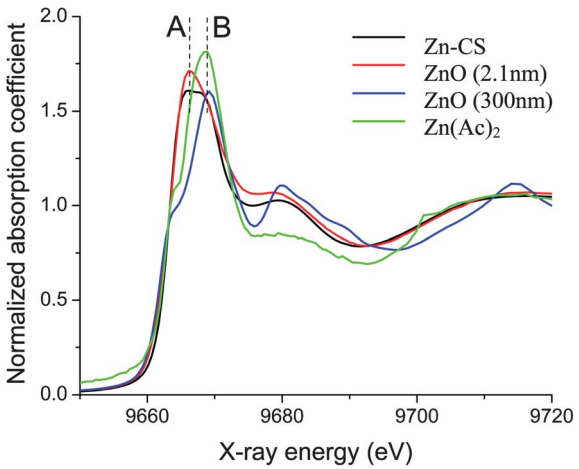

Fig. 2 Zn K-edge XANES data in Zn–CS complex, $Zn(AC)_2$, ZnO (2.1 nm) and ZnO (300 nm) particles. The similarity between Zn–CS and ZnO (2.1 nm) is evident in the main 1s–4p transition region (peaks A and B) and beyond.

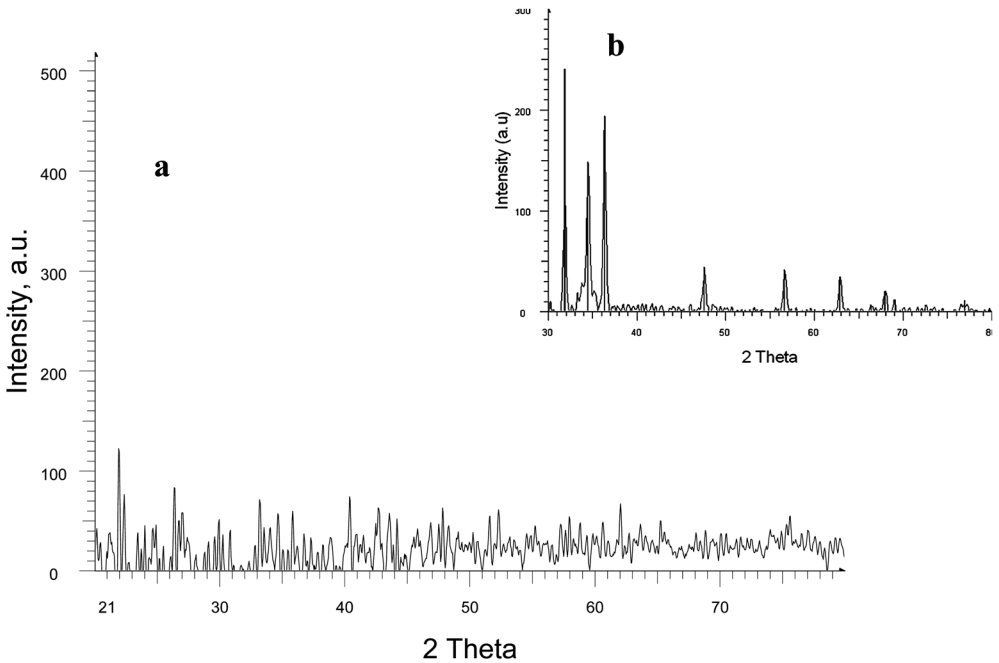

Fig. 1 XRD pattern of: (a) the powder collected after the sonochemical reaction of dissolved CS and zinc acetate solution; (b) powder collected after the sonochemical reaction of zinc acetate.

 This journal is © The Royal Society of Chemistry 2013

Published on 04 February 2013 on http://pubs.rsc.org | doi:10.1039/C3TB00555K
Downloaded by BNL Research Library on 25 March 2013

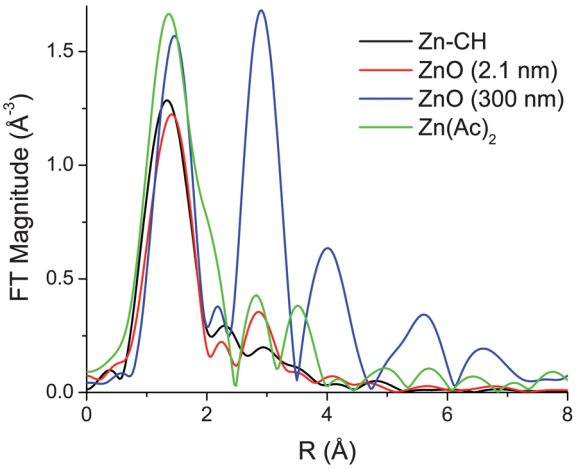

Fig. 3 Fourier transform magnitudes of EXAFS data in the 4 compounds described in Fig. 2.

position of $Zn(Ac)_2$ were similar to those observed in bulk ZnO, since in both of them ZnO is in the tetrahedral configuration.[23] The shape and position of the main absorption peak in the Zn–CS composite (Fig. 2) are very similar to those in ZnO (2.1 nm), while very different from either bulk ZnO or $Zn(Ac)_2$. Hence, we suggest that the Zn–CS complex contains low dimensional (several nm in size) ZnO crystals that are possibly too disordered and/or too small to be detected by XRD.

To verify this hypothesis, we compared EXAFS data for the same systems shown in Fig. 2. In agreement with our hypothesis drawn from examining the data in Fig. 2, the local structure in the first coordination shell of $Zn(Ac)_2$ appears similar to that in 300 nm ZnO (Fig. 3). The similarity between Zn–CS and 2.1 nm ZnO is also evident in the first peak region, supporting the XANES data. The fact that the Zn–CS composite is not so structured in the more distant shells around Zn as compared to the 2.1 nm ZnO nanoparticles indicates that the size of ZnO in the Zn–CS complex is smaller than 2.1 nm and/or the system is more disordered.

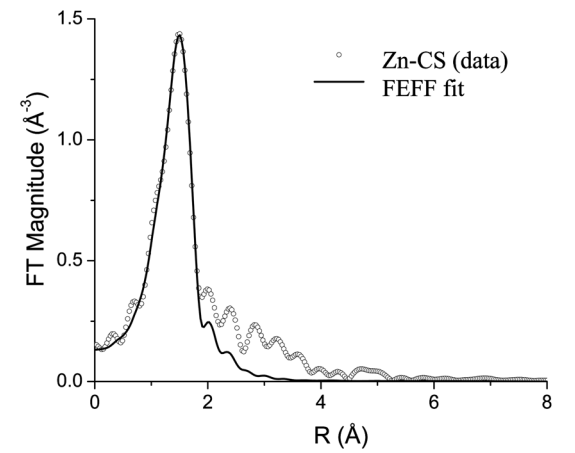

Fig. 4 Fourier transform magnitudes of the EXAFS data and fit for the Zn–CS complex.

Table 1 Results of the first shell EXAFS data analysis in the Zn–CS system. The reference data obtained by a similar analysis for bulk ZnO and 2.1 nm ZnO particles are from ref. 21

Sample	N_{Zn-O}	R_{Zn-O} (Å)	$\sigma_{Zn-O}{}^2$ (Å^2)
ZnO bulk [ref. 21]	4(fixed)	1.970(7)	0.0040(10)
ZnO 2.1 nm [ref. 21]	3.9(1.1)	1.959(25)	0.004(3)
Zn–CS	4.5(7)	1.990(16)	0.0071(24)

We have further quantitatively analyzed the collected data to find conclusive evidence for the Zn–CS complex formation. Zn K-edge EXAFS data were analyzed using the IFEFFIT data analysis program.[24] Theoretical model for FEFF calculation[25] was constructed using atomic coordinates from the bulk ZnO structure. The coordination number of the Zn–O bond, the Zn–O distance and its mean square disorder were varied in the fit. The passive electron reduction factor was found from the fit to bulk Zn foil and fixed in the analysis to be equal to 0.86. Fig. 4 shows the data and the fit in *r*-space, whereas the best fit results are presented in Table 1. Data for the bulk and nanocrystalline ZnO were analyzed under the same conditions as the Zn–CS complex and are shown for comparison. The coordination numbers and bond lengths are similar among the three systems, within uncertainties, although the largest Zn–O distance is in the Zn–CS complex. We are not ruling out the

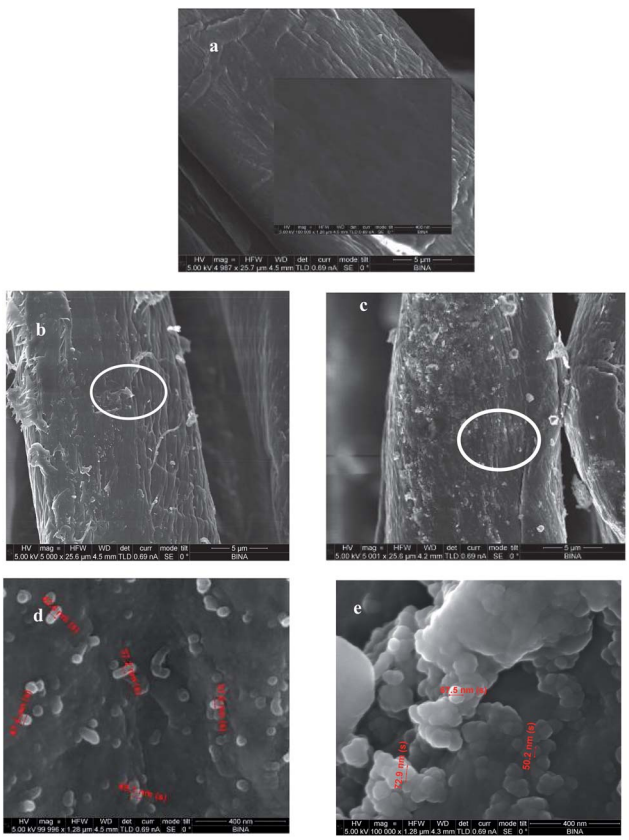

Fig. 5 ESEM images of: (a) pristine cotton fabric (MAGX5K); inset image at MAGX100K; (b) cotton coated with CS (MAGX5K); (c) cotton coated with the Zn–CS complex (MAGX5K); (d) a selected area on (b) at MAGX100K; and (e) a selected area on (c) at MAGX100K.

Published on 04 February 2013 on http://pubs.rsc.org | doi:10.1039/C3TB00555K
Downloaded by BNL Research Library on 25 March 2013

possibility that this elongation is caused by the presence of chitosan in the first coordination sphere, however, the lack of a well-defined structure beyond the first shell precludes the quantitative investigation of this possibility. By self-consistently interpreting the results from the long- (XRD) and short-range (XANES and EXAFS) methods, we conclude that the nature of Zn in the Zn–CS complex is predominantly a nanocrystalline ZnO, with the average particle size of less than 2 nm.

3.1.3 Morphology of the coating. Fig. 5a and b show the SEM images of the pristine and the CS-coated cotton, respectively, while Fig. 5d shows a selected region from Fig. 5b scanned under a higher magnification in order to study the morphology of the coating. A dense layer of spherical and rod-like CS NPs with a particle diameter of around 40 nm is observed on the fibers.

The morphology of the fibers treated in the presence of chitosan and Zn^{2+} solution is shown in Fig. 5c, while Fig. 5e represents a higher magnification image of Fig. 5c. Again, a dense layer of spherical NPs ranging from 50 to 70 nm was observed on the fibers. According to the structural characterization no individual ZnO and CS nanoparticles can be distinguished. To determine the concentration of Zn^{2+} ions on the fabric treated with CS and Zn, the coating was dissolved in acetic acid, and the solution was analyzed by ICP. The amount of Zn on the surface was estimated to be 0.19 wt%. The XRD and ESEM surface characterization of the cotton sample sonicated in the presence of CS and $Zn(AC)_2$ support the hypothesis that the coating consists of a combination of CS and Zn. Both components were found in the dense coating layer of NPs.

Table 2 Atomic concentration from the XPS analysis

Sample	N atomic concentration (%)	Zn atomic concentration (%)
CS	6.59	—
Zn–CS	5.59	0.21

3.2 Surface composition of the coated fabric

XPS studies were carried out in order to obtain an indication of the deposition of CS or the Zn–CS complex on the surface of the fabrics. In addition, the atomic concentration of the elements

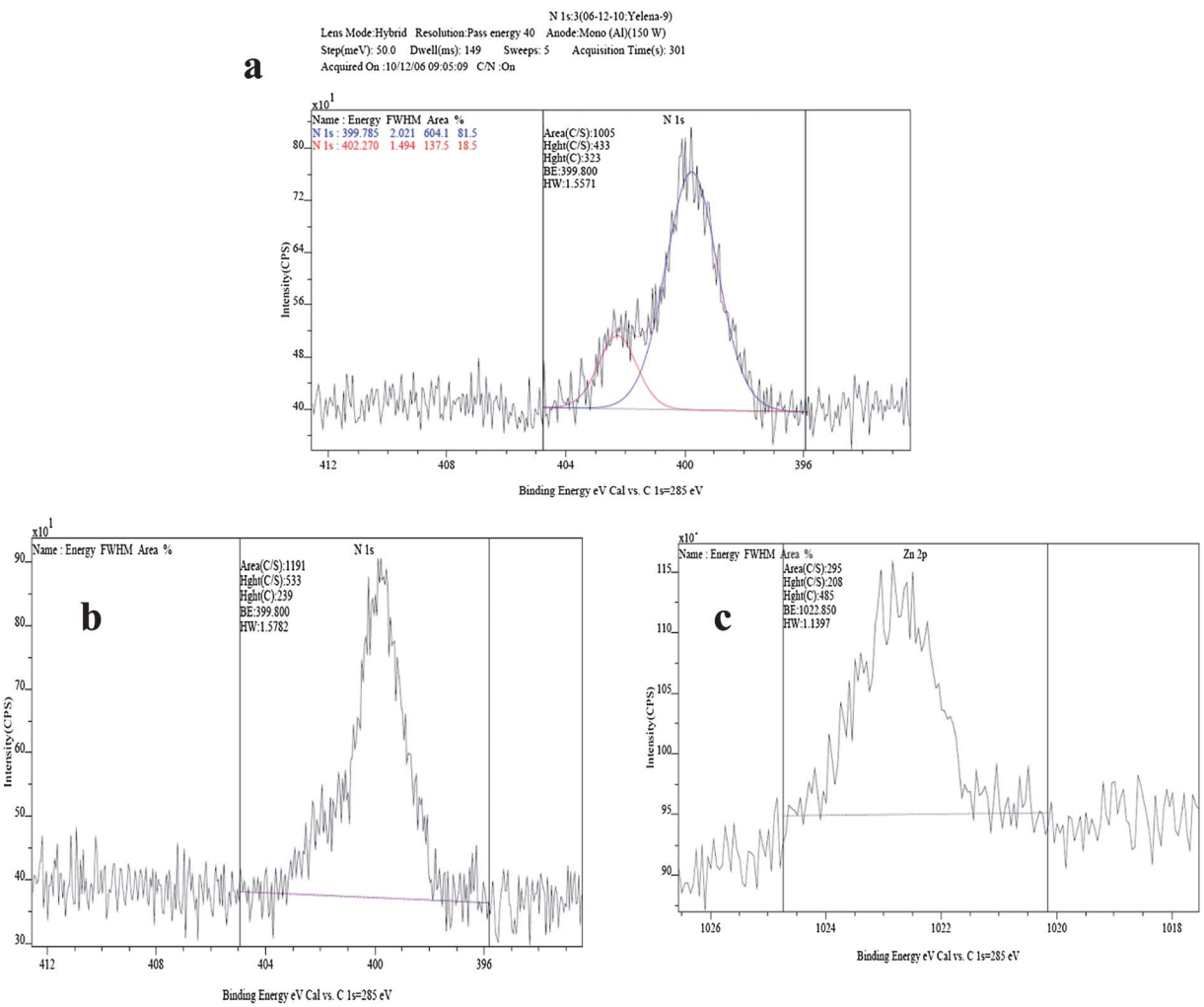

Fig. 6 N and Zn XPS spectra of cotton sonicated in the presence of: (a) CS; (b and c) CS and $Zn(AC)_2$.

 This journal is © The Royal Society of Chemistry 2013

Published on 04 February 2013 on http://pubs.rsc.org | doi:10.1039/C3TB00555K
Downloaded by BNL Research Library on 25 March 2013

was derived from the XPS measurement (Table 2). The surface composition of the cotton sample before the sonochemical deposition consisted only of C, O and H, while on the surface of the CS-coated fabric the presence of N was also detected (Fig. 6a). An increase in the N and Zn contents on the cotton treated with both CS and zinc acetate was observed (Fig. 6b and c). The N 1s in the XPS spectrum of chitosan were evidence for the presence of amino groups with a binding energy of 399.9 eV (Fig. 6a). The second peak at 401.9 eV (Fig. 6a) was assigned to the protonated amino groups (NH_3^+) from chitosan.[26,27] The decrease of intensity of the N peak at 401.9 eV (Fig. 6b) can be attributed to the formation of the Zn–CS hybrid by complexation between Zn and chitosan amino groups.

Assuming the molecular weights of CS and Zn–CS are similar, the atomic percentages in Table 2 represent the weight percentages of the two compounds. The weight percentage of ZnO on the cotton measured by the XPS is very close to the concentration obtained by the ICP measurements. This indicates that nearly all the zinc is found in the 10 nm surface depth scanned by the XPS.

3.3 FTIR analysis

The Zn–CS composite sonochemically deposited on the cotton substrate was further characterized by FTIR (Fig. 7a) and compared to the FTIR spectra of the pristine cotton (Fig. 7c), and the cotton coated with CS (Fig. 7b). The FTIR spectrum of the cotton coated with CS was very similar to the spectrum of cotton alone. The only distinct difference was the band at 1631 cm^{-1} which is characteristic for the amino groups from chitosan.[28] Some noticeable differences, however, have been observed in the spectra of Zn–CS (Fig. 7a) and CS coated cotton (Fig. 7b). Namely, the peak at 3420 cm^{-1} corresponding to the stretching vibration of –OH and $–NH_2$ became broader and of higher intensity indicating some interaction between these groups and ZnO.[29,30] The bands near 1070 cm^{-1} in pure CS are usually attributed to the C–O and C–N stretching vibrations.[30,31] The intensity of these characteristic bands significantly increased in the spectrum of the Zn–CS complex, indicating that C–O and C–N groups are involved in Zn coordination. The new bands appearing in the spectrum of Zn–CS in the range of 590–560 cm^{-1} can be attributed to the stretching vibration of N–Zn and O–Zn.[32,33] Thus, both FTIR data and XANES/EXAFS results indicated the formation of a Zn–CS complex during the sonochemical irradiation of zinc acetate in chitosan-containing solution and its simultaneous deposition on the textile substrate.

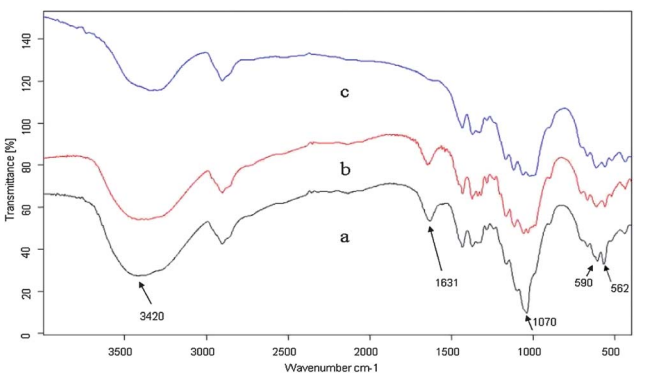

Fig. 7 FTIR spectra of the Zn–CS composite deposited on cotton: (a) Zn–CS composite; (b) CS alone; and (c) pristine cotton.

3.4 Mechanism of sonochemical deposition of chitosan and the chitosan–Zn composite on textiles

In a first set of experiments, CS dissolved in 1% aqueous acetic acid (pH ~ 4) was deposited alone on the cotton fabric. After starting the sonication, the pH of the solution was adjusted to 8 by dropwise addition of ammonia. The alkaline medium converts CS into its non-protonated insoluble form. CS NPs were simultaneously formed and precipitated under sonication on the fabric (see the size and shape of CS in Fig. 5b and d). The phenomenon of using sonochemistry for coating substrates is well studied and described elsewhere.[18–20] Briefly, the sonochemical irradiation of a liquid causes two primary effects, namely, cavitation (bubble formation, growth, collapse) and heating. When the microscopic cavitation bubbles collapse near the surface of the solid substrate, they generate powerful shock waves and microjets that cause effective stirring/mixing of the adjacent liquid layer. The after-effects of the cavitation are several hundred times greater in heterogeneous systems than in homogeneous systems. In our case, the ultrasonic waves promote the fast migration of the newly formed CS NPs to the fabrics' surface. The collision of the impinging NPs with the solid surface might cause a local "fusion" with the fibers at the contact sites, which may be the reason why the particles strongly adhere to the fabric. The sonochemical coating is actually based on physical interactions and not on chemical bonding of the coating to the substrate.

In a second set of experiments, $Zn(Ac)_2$ solution was added to the dissolved CS. The pH of the solution was adjusted to 8 and the solution was further sonicated. Under these conditions two separate processes may occur, namely, formation of CS NPs (as above) and formation of ZnO NPs.[20] However, the phenomenon of CS–Zn complexation is well known[33] and while exposing the Zn^{2+} ions to chitosan solution a CS–Zn^{2+} complex is formed. Following the adjustment of the pH to 8, ZnO NPs are formed and are bonded to chitosan. This experiment for simultaneous deposition of CS and ZnO revealed synergistic enhancement of the antibacterial activity of the chitosan coated fabrics.

The concept described in the current paper can be regarded as a general approach for synthesis of organic and metal–organic nanoparticles using a sonochemical method. Importantly, the previous knowledge on the simultaneous sonochemical formation and deposition of inorganic NPs on textile surfaces has been extended and includes now: (i) organic NPs and (ii) organic–inorganic hybrid NPs. Moreover, these NPs are generated and applied as coatings in a single-step sonochemical process. The purpose of creating an organic coating built of NPs of antimicrobial biopolymers is to achieve even higher antimicrobial activity due to the large surface area of the active phase, coupled to the low amount of the coating material. Although

Published on 04 February 2013 on http://pubs.rsc.org | doi:10.1039/C3TB00555K
Downloaded by BNL Research Library on 25 March 2013

not considered as the main goal of the current paper, a general technique for the formation of organic NPs from organic materials solution was developed.

3.5 Antibacterial activity

The results of the antibacterial efficacy testing for the coated fabrics are shown in Fig. 8. According to the BS EN ISO 20743 standard[34] used for the antibacterial efficacy tests, only levels greater than 2 log can be considered as indicating an antibacterial effect. The antibacterial activity of the CS treated cotton is rather low against *E. coli* ($A < 1$ log), but satisfactory against *E. faecalis* ($A > 2$ log). In contrast, the Zn–CS composite coating displayed very good levels of antibacterial activity against both *E. coli* and *E. faecalis* ($A > 4$ log).

Differences in the antibacterial activity of CS against different species of bacteria have been already reported.[35,36] Here again the Gram-negative bacteria *E. coli* was less affected by CS than the Gram positive bacteria *E. faecalis*. One mechanism through which CS is believed to exert its antibacterial effect is *via* perturbation of the bacterial cell membrane.[37] As CS is positively charged it can interact with the negatively charged lipidic bacterial membranes, and thus can change their permeability, ultimately effecting cell growth and viability. Since the Gram negative bacteria *E. coli* has a double outer membrane it might be less susceptible to the effects of the surface disruption than the Gram positive bacteria *E. faecalis* which only has a single membrane.

One of the goals of the current research was to increase the antibacterial activity of both chitosan and ZnO NPs. The enhanced antibacterial properties of the Zn–CS complex were deduced from the comparison with the antibacterial efficiency of the same amount of Zn alone on the fabric. From our previous studies on ZnO-coated textiles[19] we found that 0.5 wt% ZnO on the fibers sufficed for a good antibacterial effect. Nevertheless, a very low antibacterial activity was detected in the current study for fabrics coated with either 0.4 or 0.3 wt% ZnO. Less than 2 log reduction of bacterial growth was measured for the sample coated with 0.4 wt% ZnO, while no killing of bacteria was achieved with 0.3 wt% ZnO coating. The fact that only 0.18 wt% ZnO incorporated in the hybrid Zn–CS NPs coating decreased the bacterial growth by log 4 demonstrates the superiority of the biopolymer–metal oxide complex over the coating containing a similar amount of ZnO NPs alone. This enhanced antibacterial effect is partially due to the incorporation of ultra-small ZnO NPs (2.1 nm) in the composite coating. It should be pointed out that our previous and current attempts to reduce the ZnO particle size were not successful due to NP aggregation. Particles no smaller than 30 nm were obtained by varying sonochemical parameters such as temperature, sonication time, concentration of $Zn(Ac)_2$, and ultrasonic power. In the current study, the use of CS assisted the formation of 2.1 nm size ZnO particles. As a consequence of the ultra-small particle size, ZnO coating of only 0.18 wt% efficiently killed bacteria.

Generally, ZnO displays a broad spectrum of antibacterial activity through a number of mechanisms including the production of reactive oxygen species and membrane disruption.[38,39] Taking into account the mechanism that requires contact of ZnO with moisture, the hydrophilicity of CS favors the moisture uptake unlike the hydrophobic ZnO. Finally, enhanced biocompatibility of the CS–ZnO NPs in comparison with ZnO could be also expected due to the reduced water solubility of the CS–ZnO complex.

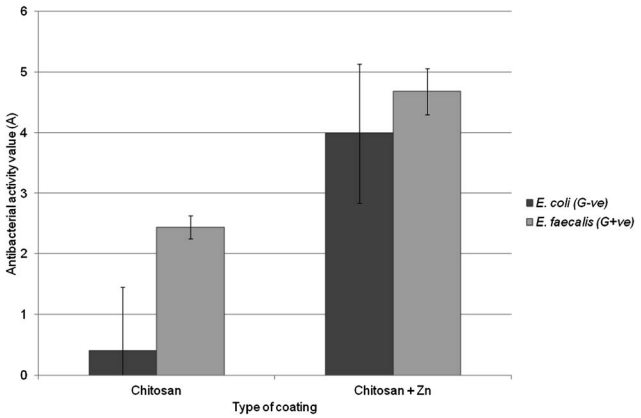

Fig. 8 Antibacterial activity values (A) for CS and Zn–CS coated cotton against *E. coli* and *E. faecalis*. The test was carried out according to the absorption method from ISO 20743:2007.

4 Conclusions

The current study presents a methodology for a one-step deposition of an organic and a metal–organic compound with intrinsic antibacterial properties on textiles. The sonochemical technique proved to be a feasible approach for producing organic NPs from soluble compounds without loss of antimicrobial properties. Physico-chemical methods of characterization revealed the *in situ* sonochemical formation of a Zn–CS complex that was subsequently deposited on the fabric surface as NPs with a size of about 60 nm. The antibacterial performance of the coated fabrics was tested against both Gram positive (*Enterococcus faecalis*) and Gram negative (*Escherichia coli*) bacteria species. The fabric coated with Zn–CS NPs showed higher levels of antibacterial activity than CS coated cotton. The existence of ultra-small ZnO NPs (less than 2.1 nm) might lead to higher antibacterial activity. In addition, the Zn–CS coating is not soluble in water and this is a clear advantage in various applications where the stability of the coating is of utmost importance.

Acknowledgements

This research was carried out as part of the activities of the SONO Consortium, contract no. NMP-2008-1.2-1 - 228730. SONO is an IP Project of the 7th EC Program. AIF acknowledges support by NSF-DMR-1006232. AP acknowledges support by U.S. Department of Energy grant no. DE-FG02-03ER15476. Beamline X18B at the NSLS is supported by the U.S. Department of Energy grant no. DE-FG02-05ER15688. We thank Sarah Mizrachi for help during synchrotron measurements.

 This journal is © The Royal Society of Chemistry 2013

Published on 04 February 2013 on http://pubs.rsc.org | doi:10.1039/C3TB00555K
Downloaded by BNL Research Library on 25 March 2013

References

1 Z. Zhang, L. Chen, J. Ji, Y. Huang and D. Chen, Antibacterial properties of cotton fabrics treated with chitosan, *Text. Res. J.*, 2003, **73**, 1103–1106.
2 T. Öktem, Surface treatment of cotton fabrics with chitosan, *Color. Technol.*, 2003, **119**, 241–246.
3 O. L. Shanmugasundaram, Chitosan coated cotton yarn and it's effect on the antimicrobial activity, *JTATM*, 2006, **5**, 1–6.
4 W. Ye, J. H. Xin, P. L. K. L. D. Lee and T. L. Kwong, Durable antibacterial finish on cotton fabric by using chitosan-based polymeric core-shell particles, *J. Appl. Polym. Sci.*, 2006, **102**, 1787–1793.
5 K. F. El-talawy, M. A. El-bendary, A. G. Elhendawy and S. M. Hudson, The antimicrobial activity of cotton fabrics treated with different crosslinking agents and chitosan, *Carbohydr. Polym.*, 2005, **60**, 421–430.
6 D. T. W. Chun and G. R. Gamble, Using the reactive dye method to covalently attach antibacterial compounds to cotton, *J. Cotton Sci.*, 2007, **11**, 154–158.
7 S.-H. Lee, M.-J. Kim and H. Park, Characteristics of cotton fabrics treated with epichlorohydrin and chitosan, *J. Appl. Polym. Sci.*, 2010, **117**, 623–628.
8 W. Fana, W. Yan, Z. Xu and N. Ni, Formation mechanism of monodisperse, low molecular weight chitosan nanoparticles by ionic gelation technique, *Colloids Surf., B*, 2012, **90**, 21–27.
9 S. Wazed Ali, M. Joshi and S. Rajendran, Novel, self-assembled antimicrobial textile coating containing chitosan nanoparticles, *AATCC Rev.*, 2011, **11**, 49–55.
10 J.-W. Rhim, S.-I. Hong, H.-M. Park and P. Y. W. Ng, Preparation and characterization of chitosan-based nanocomposite films with antimicrobial activity, *J. Agric. Food Chem.*, 2006, **54**, 5814–5822.
11 S. Saravanan, S. Nethala, S. Pattnaik, A. Tripathi, A. Moorthi and N. Selvamurugan, Preparation, characterization and antimicrobial activity of a bio-composite scaffold containing chitosan/nano-hydroxyapatite/nano-silver for bone tissue engineering, *Int. J. Biol. Macromol.*, 2011, **49**, 188–193.
12 K. Vimala, Y. M. Mohan, K. S. Sivudu, K. Varaprasad, S. Ravindra, N. N. Reddy, Y. Padma, B. Sreedhar and K. M. Raju, Fabrication of porous chitosan films impregnated with silver nanoparticles: a facile approach for superior antibacterial application, *Colloids Surf., B*, 2010, **76**, 248–258.
13 L.-H. Li, J.-C. Deng, H.-R. Deng, Z.-L. Liu and X.-L. Li, Preparation, characterization and antimicrobial activities of chitosan/Ag/ZnO blend films, *Chem. Eng. J.*, 2010, **160**, 378–382.
14 L.-H. Li, J.-C. Deng, H.-R. Deng, Z.-L. Liu and L. Xin, Synthesis and characterization of chitosan/ZnO nanoparticle composite membranes, *Carbohydr. Res.*, 2010, **345**, 994–998.
15 R. Salehi, M. Arami, N. M. Mahmoodi, H. Bahrami and S. Khorramfar, Novel biocompatible composite (chitosan–zinc oxide nanoparticle): preparation, characterization and dye adsorption properties, *Colloids Surf., B*, 2010, **80**, 86–93.
16 A. El. Shafei and A. Abou-Okeil, ZnO/carboxymethyl chitosan bionano-composite to impart antibacterial and UV protection for cotton fabric, *Carbohydr. Polym.*, 2011, **83**, 920–925.
17 A. Becheri, M. Durr, P. L. Nostro and P. Baglioni, Synthesis and characterization of zinc oxide nanoparticles: application to textiles as UV-absorbers, *J. Nanopart. Res.*, 2008, **10**, 679–689.
18 I. Perelshtein, G. Applerot, N. Perkas, G. M. Guibert, S. Mikhailov and A. Gedanken, Sonochemical coating of silver nanoparticles on textile fabrics (nylon, polyester and cotton) and their antibacterial activity, *Nanotechnology*, 2008, **19**, 245705.
19 I. Perelshtein, G. Applerot, N. Perkas, E. Wehrschetz-Sigl, A. Hasmann, G. M. Guebitz and A. Gedanken, Antibacterial properties of an *in situ* generated and simultaneously deposited nanocrystalline ZnO on fabrics, *ACS Appl. Mater. Interfaces*, 2009, **1**, 361–366.
20 I. Perelshtein, G. Applerot, N. Perkas, E. Wehrschuetz-Sigl, A. Hasmann, G. Guebitz and A. Gedanken, CuO–cotton nanocomposite: formation, morphology, and antibacterial activity, *Surf. Coat. Technol.*, 2009, **204**, 54–57.
21 A. Patlolla, J. Zunino III, A. I. Frenkel and Z. Iqbal, Thermochromism in polydiacetylene-metal oxide nanocomposites, *J. Mater. Chem.*, 2012, **22**, 7028–7035.
22 A. Kuzmin, S. Larcheri and F. Rocca, Zn K-edge XANES in nanocrystalline ZnO, *J. Phys.: Conf. Ser.*, 2007, **93**, 012045.
23 M. Tokumoto, V. Briouis, C. Santilli and S. Pulcinelli, Preparation of ZnO nanoparticles: structural study of the molecular precursor, *J. Sol-Gel Sci. Technol.*, 2003, **26**, 547–551.
24 B. Ravel and M. Newville, ATHENA, ARTEMIS, HEPHAESTUS: data analysis for X-ray absorption spectroscopy using IFEFFIT, *J. Synchrotron Radiat.*, 2005, **12**, 537–541.
25 S. I. Zabinsky, J. J. Rehr, A. Ankudinov, R. C. Albers and M. Eller, Multiple-scattering calculations of X-ray-absorption spectra, *Phys. Rev. B: Condens. Matter Mater. Phys.*, 1995, **52**, 2995–3009.
26 H. J. Martin, K. H. Schulz, J. D. Bumgardner and K. B. Walters, XPS study on the use of 3-aminopropyltriethoxysilane to bond chitosan to a titanium surface, *Langmuir*, 2007, **23**, 6645–6651.
27 Y. Yan, B. Hao and G. Chen, Biomimetic synthesis of titania with chitosan-mediated phase transformation at room temperature, *J. Mater. Chem.*, 2011, **21**, 10755–10760.
28 A. D. Gross and R. A. Jones, in *An introduction to practical infra-red spectroscopy*, Butterworth, London, 1969, p. 102.
29 X. Wang, Y. Du and H. Liu, Preparation, characterization and antimicrobial activity of chitosan–Zn complex, *Carbohydr. Polym.*, 2004, **56**, 21–26.
30 R. Salehi, M. Arami, N. M. Mahmoodi, H. Bahrami and S. Khorramfar, Novel biocompatible composite (chitosan–zinc oxide nanoparticle): preparation, characterization and dye adsorption properties, *Colloids Surf., B*, 2010, **80**, 86–93.
31 D. S. Vicentini, A. Smania Jr and M. C. M. Laranjeira, Chitosan/poly(vinyl alcohol) films containing ZnO nanoparticles and plasticizers, *Mater. Sci. Eng., C*, 2010, **30**, 503–508.

32 L.-G. Tang and D. N.-S. Hon, Chelation of chitosan derivatives with zinc ions. II. Association complexes of Zn^{+2} onto *O*,*N*-carboxymethyl chitosan, *J. Appl. Polym. Sci.*, 2001, **79**, 1476–1485.
33 X. Wang, Y. Du and H. Liu, Preparation, characterization and antimicrobial activity of chitosan–Zn complex, *Carbohydr. Polym.*, 2004, **56**, 21–26.
34 Anonymous, *Textiles – Determination of Antibacterial Activity of Antibacterial Finished Products*, British Standards Institution, 2007, BS EN ISO 20743:2007(E).
35 L.-Y. Zheng and J.-F. Zhu, Study on antimicrobial activity of chitosan with different molecular weights, *Carbohydr. Polym.*, 2003, **54**, 527–530.
36 R. C. Goy, D. de Britto and O. B. G. Assis, A review of the antimicrobial activity of chitosan, *Polim.: Cienc. Tecnol.*, 2009, **19**, 241–247.
37 M. Kong, X. G. Chen, K. Xing and H. J. Park, Antimicrobial properties of chitosan and mode of action: a state of the art review, *Int. J. Food Microbiol.*, 2010, **144**, 51–63.
38 G. Applerot, A. Lipovsky, R. Dror, N. Perkas, Y. Nitzan, R. Lubart and A. Gedanken, *Adv. Funct.Mater.*, 2009, **19**, 842–852.
39 Y. Xie, Y. He, P. L. Irwin, T. Jin and X. Shi, Antibacterial activity and mode of action of ZnO, *Appl. Environ. Microbiol.*, 2011, **77**, 2325–2331.

Published on 04 February 2013 on http://pubs.rsc.org | doi:10.1039/C3TB00555K
Downloaded by BNL Research Library on 25 March 2013

This journal is © The Royal Society of Chemistry 2013